Article

Wind Microturbine with Adjustable Blade Pitch Angle

Stanisław Chudzik

Faculty of Electrical Engineering, Czestochowa University of Technology, 42-200 Czestochowa, Poland; stanislaw.chudzik@pcz.pl

Abstract: The article presents the results of research on the operation of a wind microturbine model with an adjustable blade pitch angle. The physical basics of wind turbine operation and the methods of its optimal control are discussed. The results of the measurements carried out for the selected blade geometry with the possibility of adjusting the pitch angle are presented. The tests were carried out for a resistive load with a linear characteristic and for a load with a non-linear characteristic of a Li-Po battery. The results of the operation of a simple MPPT control algorithm are presented. The practical methods of controlling larger wind turbines are not optimal for small and very small turbines. The conducted research focused on determining the possibility of using blades with an adjustable angle setting, depending on the rotational speed in wind microturbines. The use of a simple mechanism for changing the pitch angle of the blades depending on the rotational speed of the turbine can increase the efficiency of the microturbine in a wider range of wind speeds.

Keywords: small wind turbine control; maximum power point tracking; pitch angle wind turbine

1. Introduction

The power of designed and built wind farms in the world is constantly increasing and reaches the value of MW. This pursuit is economically justified as larger turbines achieve higher efficiency of generated power. Modern commercial wind farms mostly have a horizontal axis of rotation and a three-blade turbine. The most frequently used generators are asynchronous machines and synchronous machines with permanent magnets (PMSG) together with power electronic converters and control systems. Modern wind turbines with a horizontal axis of rotation are usually adapted to work at wind speeds not exceeding 25 m/s. These turbines achieve their rated power at wind speeds between 10 and 15 m/s [1]. PMSG generators made of neodymium magnets are most often used in low-power wind turbines with high rotational speed, while in larger power plants, induction generators with a mechanical gear are used [2]. In modern wind turbines, several methods of adjusting the rotor speed and the generator power related to it are used in several ways, depending on the instantaneous wind speed [2]. To reduce mechanical power on the shaft in large turbines, pitch control is used, while in small and medium-sized ones, mainly passive stall control is used, breaking the laminar air stream [3,4].

The European Parliament issued a directive 2010/31/UE on the energy performance of buildings, introducing the nearly zero-energy building concept (zero-energy building). According to this directive, new buildings must meet the requirement that a significant amount of energy comes from renewable sources, including sources integrated with the building [5]. As a result, there is a growing interest in micro wind turbines that would supplement the electricity demand of small households [6–8]. The manufacturers' offer includes wind microturbines with a nominal power from 100 W to several kW. Miniature wind turbines can also often be seen on small yachts, recreational plots, and street-lighting lamps where there is no access to the power grid—Figure 1. Typically, such microturbines have three or more blades with as simple a profile as possible, are easy to manufacture, and directly mounted on the PMSG generator axis. Most often, the rated voltage of the generator is selected so that it charges the battery using an ordinary 6D rectifier.

(a) **(b)**
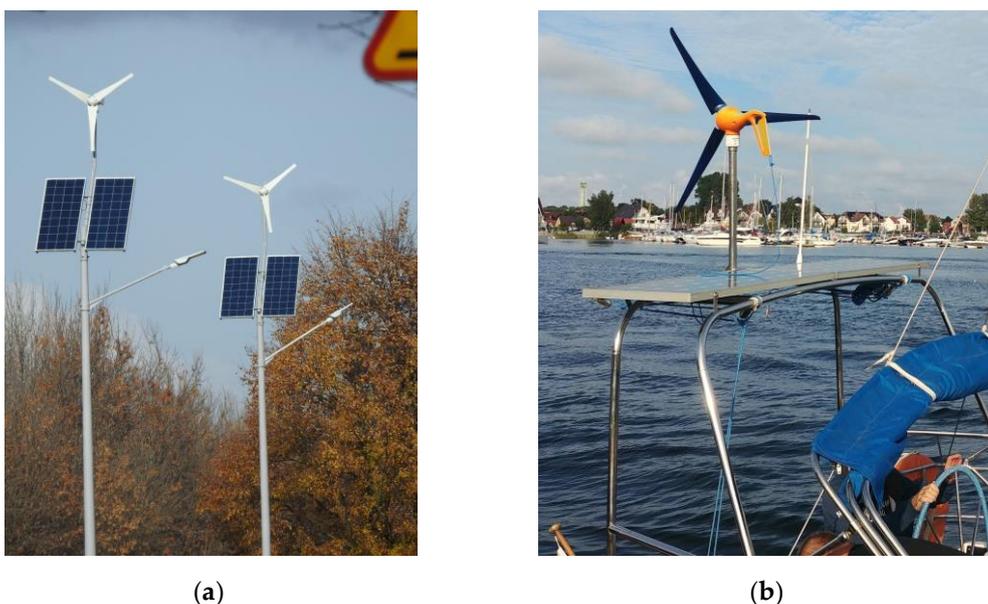
Figure 1. Hybrid power supply from renewable energy sources: (**a**) street-lighting lamp; (**b**) on the yacht.

The belief that the cost of manufacturing a controller for the optimal operation of a microturbine is high in relation to the possible improvement of the efficiency of the microturbine means that there is no such controller on the market. In addition, control methods for larger wind turbines are not optimal for small turbines [9–11]. Therefore, the author designed and built a small test stand that allows for preliminary research related to the selection of the optimal wind turbine geometry, and the development and testing of the operation of the control algorithm for the operation of a simple converter charging the battery so as to optimally use the power of the wind turbine [12].

The presented research focuses mainly on determining the possibility of using wind turbines with an adjustable blade pitch angle depending on the rotational speed in microturbines. In larger wind turbines, changing the pitch angle is only used to limit their power at high wind speeds [10,11]. Currently, such solutions in micro wind farms are not used for economic reasons. Wind microturbines are very often located in places where wind conditions are unfavorable: low height from the ground, and terrain obstacles limiting the speed of the wind stream and causing its turbulence [1,9]—Figure 1a. The use of a simple blade pitch angle adjustment mechanism depending on the angular velocity of the turbine can increase its efficiency in a wider range of wind speeds.

The test stand with small dimensions enables quick and cheap development of initial prototypes of turbine blades due to the use of 3D printing technology.

2. Materials and Methods

2.1. Working Principle of Wind Turbine

The operation of the wind turbine depends on the setting of the blade angle ϕ (Figure 2): it is the angle between the blade chord and the apparent wind V, being the sum of the vectors of the blade linear velocity $V_\omega = \omega \cdot r$ and the wind speed V. The value of the angle of attack α depends on the ratio of the linear blade speed V_ω to the wind speed V and the blade position angle. Two forces act on the turbine blade: the lifting force F_L, perpendicular to the direction of the resultant velocity V, and the thrust F_D, corresponding to its direction. The rotation of the turbine causes the component F_T of the resultant force F_L in the direction of the blade rotation. The value of F_T depends on the aerodynamic profile of the blade and is a non-linear function of the angle of attack. In the range of small values of the angle of attack, this force grows approximately linearly, but from a certain value of this angle it rapidly decreases; a stall state occurs [1,2,13]. Maintaining a constant value of the angle of attack, ensuring maximum aerodynamic efficiency, requires maintaining an

approximately constant ratio of the angular velocity of the rotor to the wind speed, i.e., the change in rotor speed in proportion to the wind speed.
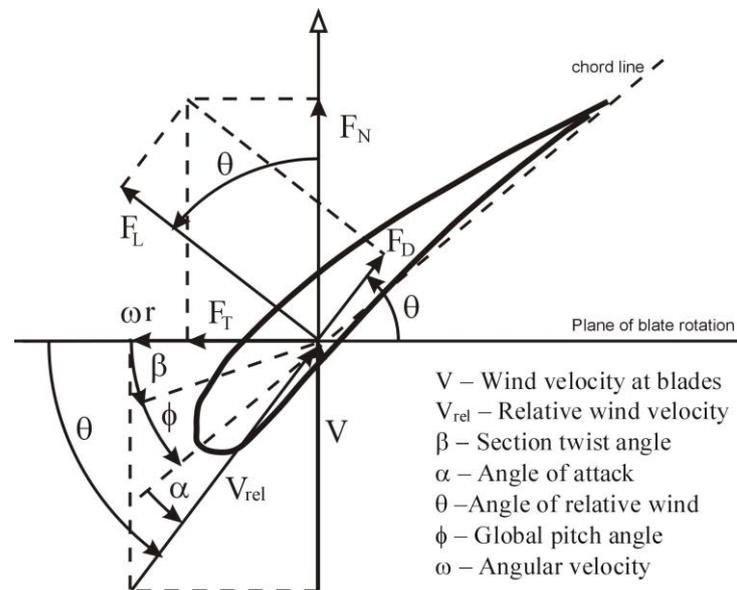
Figure 2. Aerodynamic forces on the blade profile.

The lift generated by the airfoil section is a function of the angle of attack to the incoming air stream. The angle of the air stream inflow depends on the rotational speed and the wind speed within a certain radius. The required twist angle of the blade depends on the ratio of the airfoil speed over a certain radius and the desired angle of attack of the airfoil. The part of the blade closer to the hub is tilted more against the wind due to the high ratio of wind speed to blade radial speed. The blade tip, on the other hand, will be almost perpendicular to the wind direction. In the case of blades with a constant angle of their setting, the optimal twist angle of the blade can be determined. However, when the angle of the blade is to be adjusted, the twist angle of the blade should also change. It would be too costly to build a wind turbine with variable-adjustable geometry and currently such solutions are not used in practice. Therefore, blade angle adjustment is only used in large turbines to limit their power. In the case of airplanes or helicopters where the adjustable pitch propeller is used as a drive, the blades of such propellers have a small or zero twist angle—this provides a wider speed range for effective operation of the propulsion [1,2]. For the purposes of the research on the impact of the adjustment of the blade angle on the operating efficiency range of a wind turbine, a propeller with a straight profile and a zero twist angle of the blade was made.

The aerodynamic properties of the wind turbine are determined by the power factor $Cp(\lambda, \beta)$, which depends on the tip speed ratio λ and the blade pitch angle β. The coefficient λ is defined as the ratio of the linear speed of the turbine blade tip to the wind speed,

$$\lambda = \frac{\omega_r \cdot R}{V_w},\tag{1}$$

where ω_r is the angular velocity of the turbine and R is the radius of the turbine.

The power factor corresponding to the aerodynamic efficiency of a wind turbine is given by the expression,

$$C_P = \frac{P_m}{P_w},\tag{2}$$

where P_m is the mechanical power of the turbine and P_w is the wind power:

$$P_w = 0,5\rho\pi R^2 V^3,\tag{3}$$

where ρ is the air density.

Figure 3 shows an example of the $Cp(\lambda, \beta)$ characteristic of a wind turbine. The maximum power generated by the turbine at a given wind speed V_w is achieved for the maximum value of the efficiency coefficient corresponding to a certain optimal value λ_{opt} of the tip speed ratio [1,2].
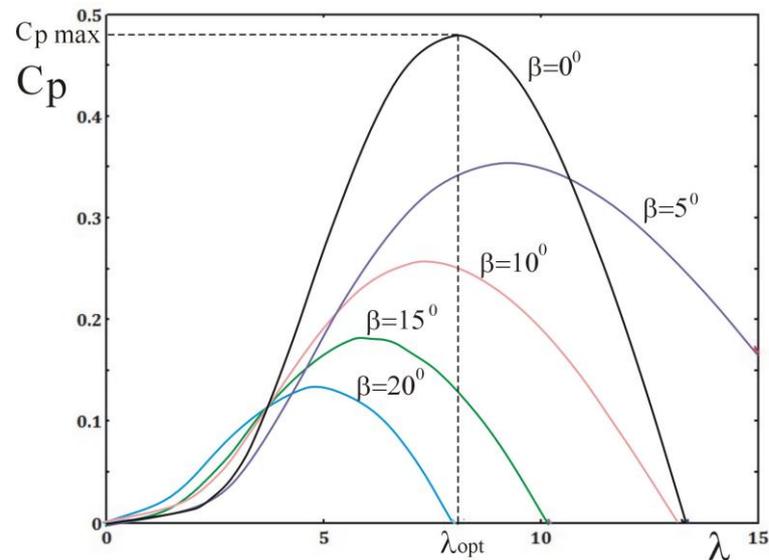
Figure 3. An example of the $Cp(\lambda, \beta)$ characteristics.

The mechanical power of the turbine and the output of the electrical system P_{out} is described by Equation (4), where M_t is the frictional moment, ω is the turbine angular velocity, J is the moment of inertia of the rotating mass, η is the overall electrical efficiency of the system from the generator input to the inverter output.

$$P_m = \frac{1}{\eta}P_{out} + \omega \cdot M_t + \omega \cdot J\frac{d\omega}{dt}, \tag{4}$$

The boundary layer is a thin layer of air and appears on the surface of objects in viscous flow. The boundary layer effect depends on the flow pattern which is related to the Reynolds number (5). Reynolds number is a function of fluid velocity,

$$Re = \frac{\rho \cdot V \cdot C}{\mu}, \tag{5}$$

where ρ is the fluid density, V is the mean velocity of the fluid, C is a chord length, and μ is the dynamic viscosity of the fluid.

Airfoil efficiency decreases as the Reynolds number decreases. Reducing the Reynolds number means that viscous effects become more dominant, increasing viscous drag. In addition, the thickness of the boundary layer will increase as the Reynolds number decreases, leading to increased shape drag or less lift. Small wind turbines usually operate at Reynolds number less than 5×10^5. In this Reynolds number range, laminar flow gets separated at the upper surface of the airfoil and is reattached to the surface as turbulent causing laminar separation bubble, which increases the drag of the airfoil. Large-scale wind turbines have become the development trend of wind power. At present, the radius of wind turbine rotors ranges to one hundred meters, or even more, which extends Reynolds number of the airfoil profile from the order of 10^6 to 10^7.

2.2. The Most Commonly Used Methods of Optimal Control of Wind Turbine Operation

The algorithms used to achieve maximum power point tracking (MPPT) by wind turbines can be divided into three main control methods: tip speed ratio (TSR) control, power signal feedback (PSF) control and, search method maximum power (hill-climb search—HCS) [14–16]. The TSR control method regulates the rotational speed of the wind turbine in order to maintain the optimal value of the tip speed ratio, at which the achieved turbine power is the highest [17,18]. This method requires measuring or estimating both the wind speed and the rotational speed of the turbine, and also requires knowledge of the characteristics of the optimal tip speed ratio for the designed turbine—Figure 4.
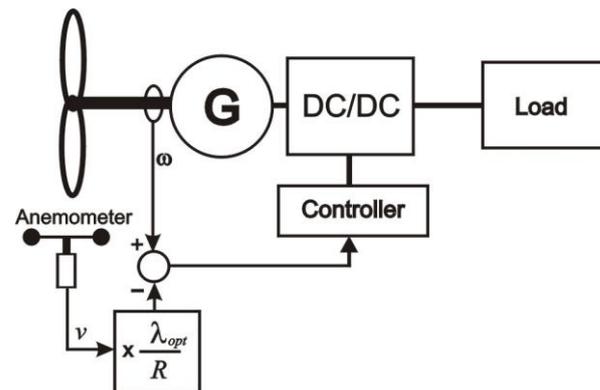

Figure 4. Tip speed ratio control.

In the PSF control method, it is required to know the maximum power characteristics of a wind turbine and to follow this curve with a control and measurement system [19,20]. The maximum power curves should be obtained by simulations or experiments with a disconnected wind turbine. In this method, the reference power is determined from the recorded maximum power curve or from the wind turbine power equation where the input speed is either wind speed or rotor speed—Figure 5.
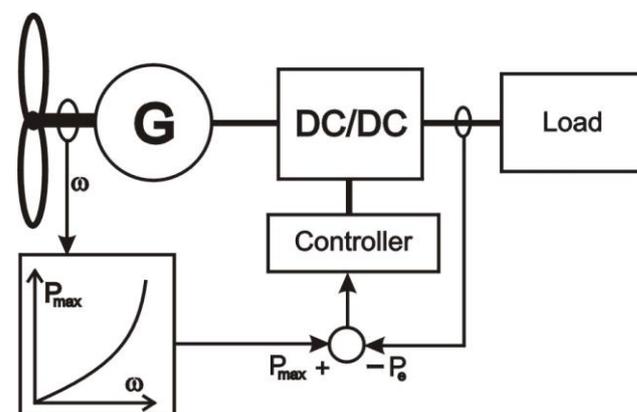

Figure 5. Power signal feedback control.

The HCS control algorithm is constantly looking for the peak power of the wind turbine—Figure 6. The tracking algorithm, depending on the position of the operating point of the turbine and the relationship between changes in power and rotational speed of the turbine, calculates the optimal signal to bring the wind turbine to the point of maximum power [21–25]. Unfortunately, HCS control can only work well when the moment of inertia of the wind turbine is very small so that the change in turbine speed occurs almost "instantaneously" to the change in wind speed. For wind turbines with higher inertia, the instantaneous power output of the power plant is related to the mechanical power of the turbine and changes in kinetic energy stored in the rotating elements, which often makes

the HCS method ineffective. HCS control does not reach the maximum power points with rapid increases in wind speed and causes the so-called "stall" when wind speed decreases, which severely limits the usefulness of this method for wind turbines. Boundary layer flow characteristics are critical for determining inputs to control systems. The occurrence of the laminar-to-turbulent transition process, especially at high angles of attack and rapid changes of angles of attack, can significantly change the aerodynamic behavior of the blade and cause the phenomenon of stalling [26,27].
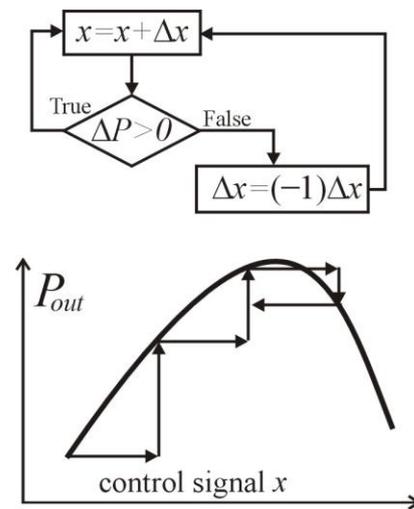
Figure 6. Hill-climb search algorithm.

It is therefore highly desirable to develop a maximum power output method for micro wind turbines that does not require measuring wind speed and turbine rotor speed, is independent of system characteristics, and is applicable to small wind turbines.

2.3. Experimental Stand

A small test stand was built for the purpose of testing the wind turbine model.

Figure 7 shows a schematic diagram of the stand. The test stand includes a virtual measurement and control device implemented on a PC class computer and a physical model of a miniature wind tunnel. The virtual measurement and control device was created in the LabView programming environment. Figure 8 shows the view of the front panel. The device can set the output value of the fan power, the value of the PWM duty cycle for the DC/DC converter, and the pitch value of the wind turbine blade. In addition, the instrument displays and records the following measured values: wind speed v, turbine speed n, generator output voltage U_G, output voltage of the DC/DC converter U_O, and load current I_O. The power delivered to the load P_O is also determined.
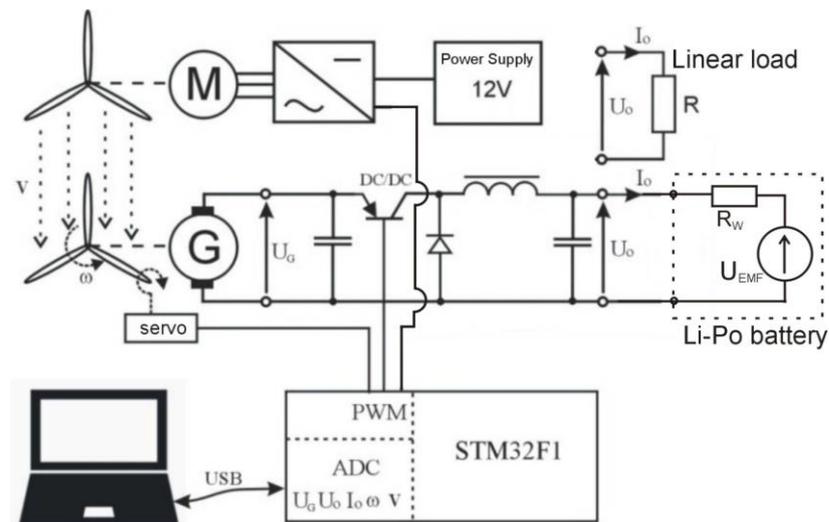
Figure 7. Schematic diagram of the stand for testing the wind microturbine model.
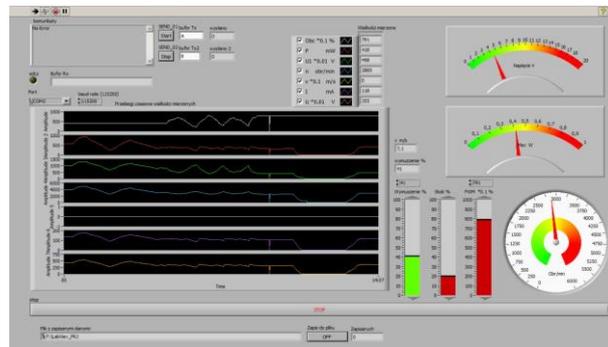

Figure 8. Virtual measuring and control device—front panel.

The model of the wind tunnel made, shown in Figure 9a,b, consists of a tunnel pipe (1) fixed in a frame (2) which also acts as a honeycomb (air stream straightener). Attached to the frame is a brushless BLDC fan motor (3) with a 203 mm (8-inch) diameter propeller and 101 mm (4-inch) pitch, and a DC brush motor (4) with permanent magnet excitation acting as a DC generator. The generator is powered by a propeller that functions as a wind turbine. At the entrance to the tunnel there is an anemometer sensor (5) measuring the speed of the wind. The BLDC motor of the fan is powered by a three-phase inverter (6). The research model has a controller (7) based on a 32-bit STM32F1 microcontroller which controls the operation of the fan, DC/DC converter, and the servomechanism (12) of the turbine propeller pitch (11). The controller also measures wind speed v, turbine rotational speed ω, generator output voltage U_G, converter output voltage U_O, and load current I_O (8). The controller, via the USB serial interface (9), communicates with the master computer on which the virtual measurement and control device program is running. The model is powered by a power supply (10) with a voltage of 12 V. Due to the small size of the model, some of its elements could be produced using a 3D printer.
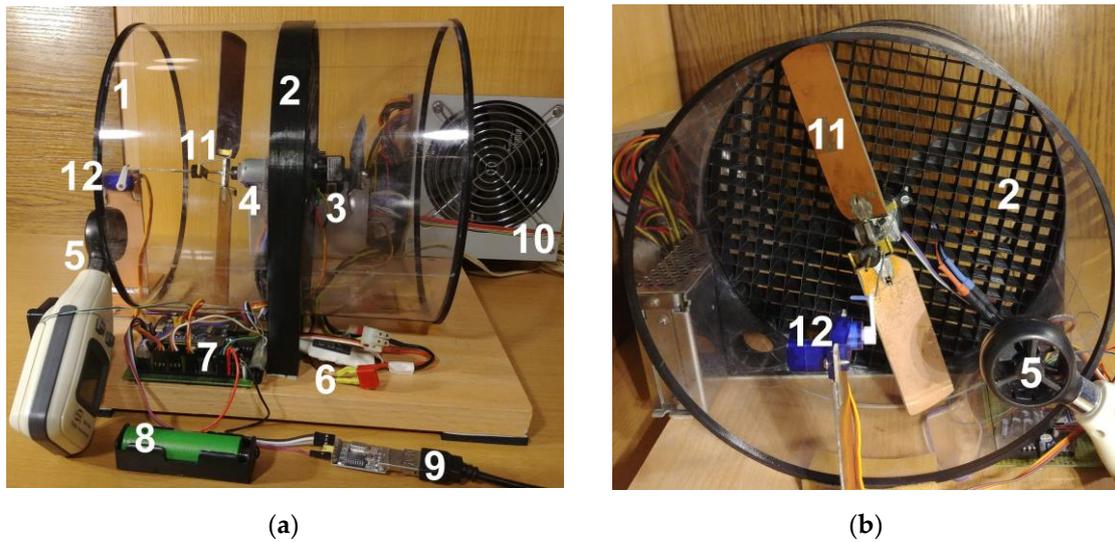
(**a**)   (**b**)

Figure 9. (**a**) View of the research model; (**b**) View of the wind tunnel.

3. Results and Discussion

The virtual measurement and control device has the ability to automatically record measured values for ten set fan power values and one hundred set values of the PWM wave fill factor for the transistor in the DC/DC converter (buck converter). Because of this solution, a matrix of 1000 values is obtained for each measured value without the tedious involvement of the person conducting the measurements and data recording. Moreover, the measuring and control device has the possibility of automatic adjustment of the blade setting angle in accordance with the control function described by the expression dependent on the measured instantaneous rotational speed of the turbine $\beta = f(n)$. Ultimately, the practical solution of the microturbine provides for a possibly simple and cheap mechanical solution using the centrifugal force of the rotating mass, which would change the pitch of the blades. The optimal control of the power plant is based on achieving the maximum power for a given wind speed value. Power control, in this system solution of the power plant, is carried out by changing the duty cycle of the PWM signal that controls the operation of the switch in a simple DC/DC converter, which has a direct impact on the value of the converter output voltage. In the conducted research, measurements were carried out for a load with a non-linear current–voltage characteristic, which is a lithium-polymer battery cell. The electromotive force EMF of the cell used, depending on the state of charge, was in the range $(3.3 \div 4.3)$ V and its internal resistance was determined as $R_w \approx 0.25$ Ω.

3.1. Wind Turbine with a Classic Aerofoil Profile Blade

In order to compare the results of the research on the influence of the adjustment of the pitch angle of the blades on the efficiency of the wind turbine operation, a propeller with a blade with a classic aerodynamic profile and a constant pitch angle was used in the experiment. Examples of power generated by a wind turbine for a resistive load as a function of the duty cycle of the PWM signal (control quantity) for different wind speeds are shown in Figure 10.
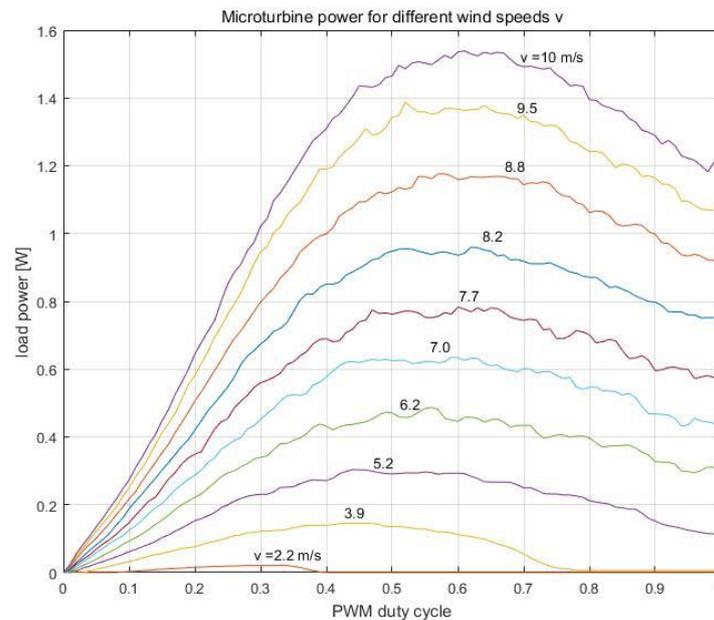
Figure 10. The power generated by a wind turbine for a linear load as a function of the control value—the duty cycle of the PWM signal, for different wind speeds.

It is worth noting that for a linear load such as a resistor, the optimal operation of the power plant for higher wind values is achieved for a narrow range of the PWM duty cycle (0.50 ÷ 0.65). The limitation of the power of the power plant in this case is mainly due to the relatively high resistance value of the generator winding. For lower wind speeds, the power limitation results mainly from the low value of mechanical power achieved by the wind turbine (propeller), which is transferred to the generator shaft. Examples of power generated by a wind turbine loaded with a Li-Po cell as a function of the duty cycle of the PWM signal (control quantity) for various wind speeds are shown in Figure 11. It is worth noting that for a non-linear load such as a Li-Po cell, the optimal control of the power plant operation requires a wider range of PWM duty cycle values within the range (0.4 ÷ 0.85). It is also necessary to take into account changes in the EMF voltage of the cell depending on the degree of its charge.
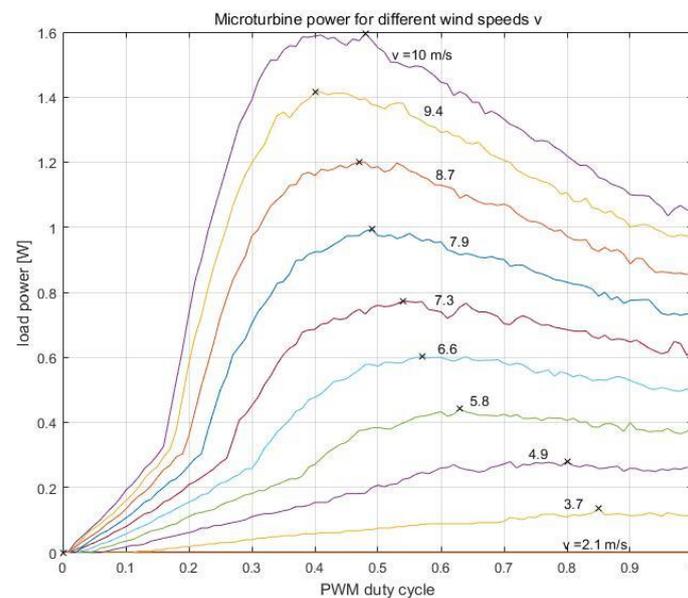
Figure 11. The power generated by a wind turbine for a non-linear load, as a function of the control value—duty cycle of the PWM signal, for different wind speeds.

Figure 12 presents the obtained characteristics of the maximum power of the power plant depending on the wind speed. It can be seen that at higher wind speeds, the slope of the characteristic no longer increases. The cause may be a significant increase in the thrust force F_r, resulting from the increase in the rotational speed of the turbine—the frontal resistance of the airfoil. In the conducted experiment, the turbine achieves a high tip speed ratio λ >10: the turbine blades are positioned almost perpendicular to the wind direction. In addition, taking into account the static friction of bearings and brushes and the cogging torque resulting from changes in the reluctance of the generator's magnetic circuit, the start-up of such a turbine is very difficult and takes place only at a relatively high wind speed of 4 m/s, compared to the wind speed of 1.5 m/s at which it stops.
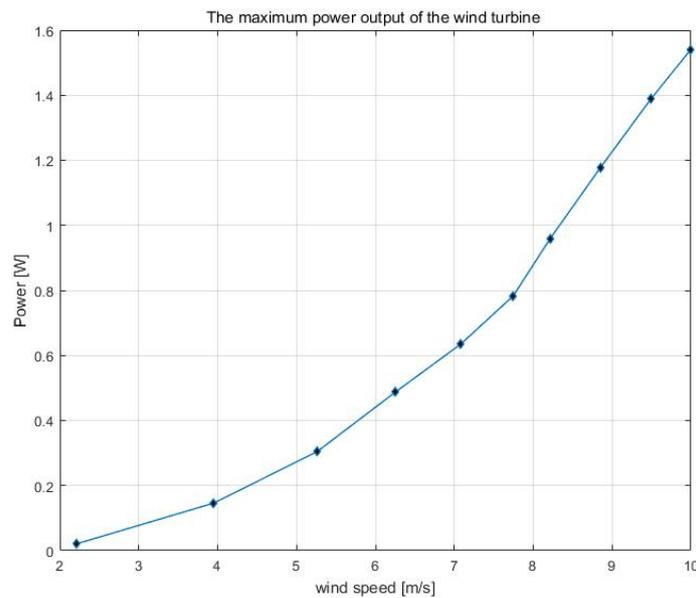
Figure 12. The maximum power of a wind turbine.

Preliminary results of the measurements indicate that the direct connection of the battery to the generator, often used in microturbines, whose charging characteristics are strongly non-linear and varies depending on the battery charge level, may be the cause of poorer efficiency of micro power plants. The solution to this problem may be the use of a possibly simple DC/DC converter, which could linearize the load characteristics of the wind microturbine.

Tests were carried out of a micro wind power plant model, controlled by a simple HCS algorithm presented in Figure 6. Figure 13 shows selected results of the experiment in the form of graphs: microturbine wind power, PWM duty factor, and turbine rotation speed. The results were obtained at a constant wind speed v = 5 m/s.
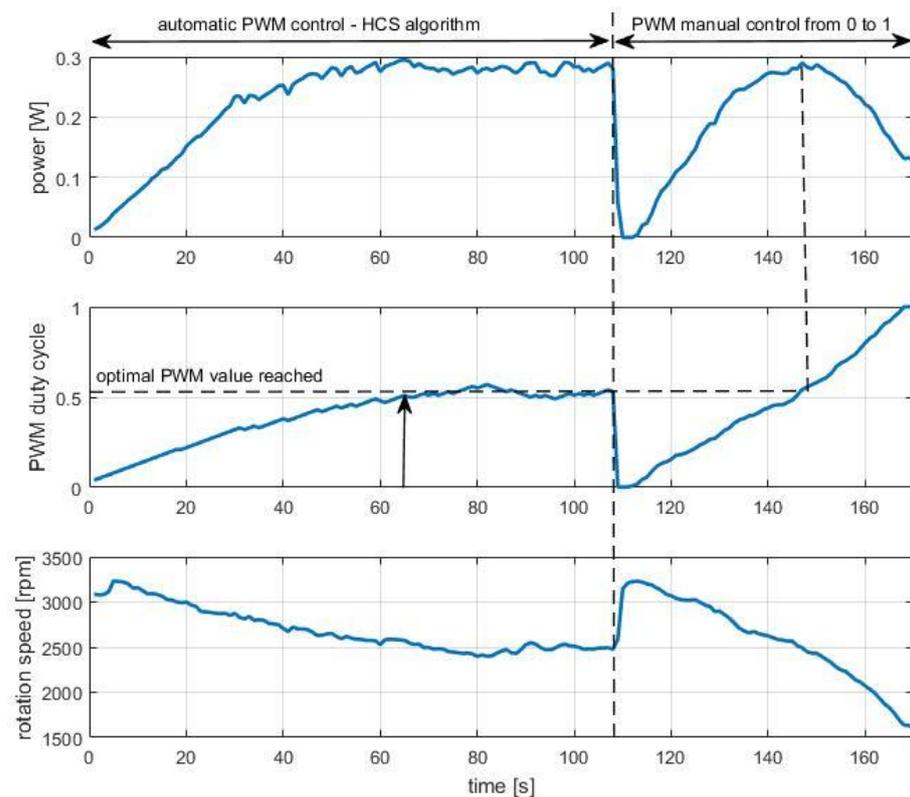
Figure 13. Graphs: microturbine power, duty factor PWM, and turbine rotation speed of a microturbine model controlled by HCS algorithm.

The results of the experiment indicate the possibility of using a simple HCS algorithm to control the operation of a wind microturbine only for a stable value of wind speed. In the case of rapid and greater decreases in wind speed, the presented simple HCS algorithm no longer works optimally, even leading to the wind turbine stopping and the need to restart it. Some improvement in operation can be achieved in this case by using the measured turbine rotational speed in the control algorithm.
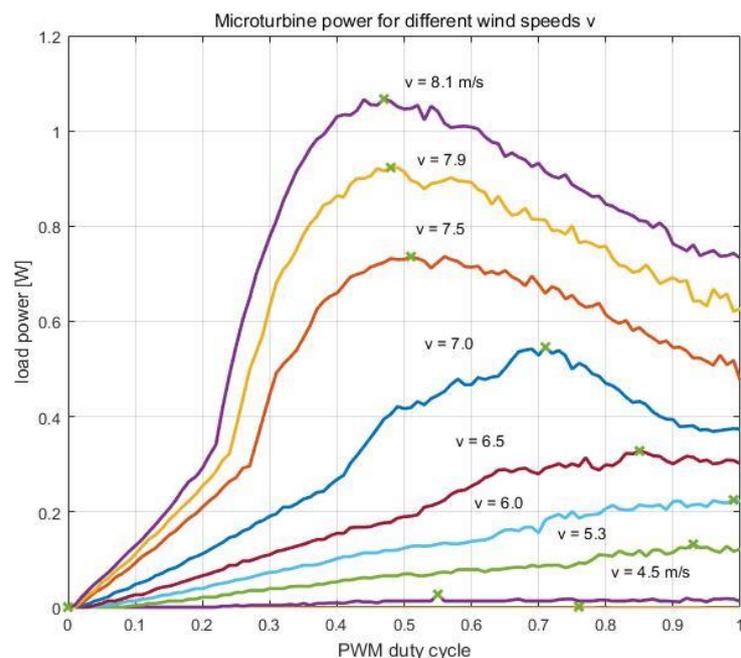
3.2. Wind Turbine with Adjustable Pitch

For the purposes of the research on the impact of the adjustment of the blade angle on the operating efficiency range of a wind turbine, a propeller with a straight profile and a zero twist angle of the blade was used in the experiment—Figure 9. Figure 14 shows the power characteristics obtained in the tests carried out on a wind turbine with a constant pitch $\beta = 15°$ as a function of the value of the PWM signal duty factor (control variable) for various wind speeds.
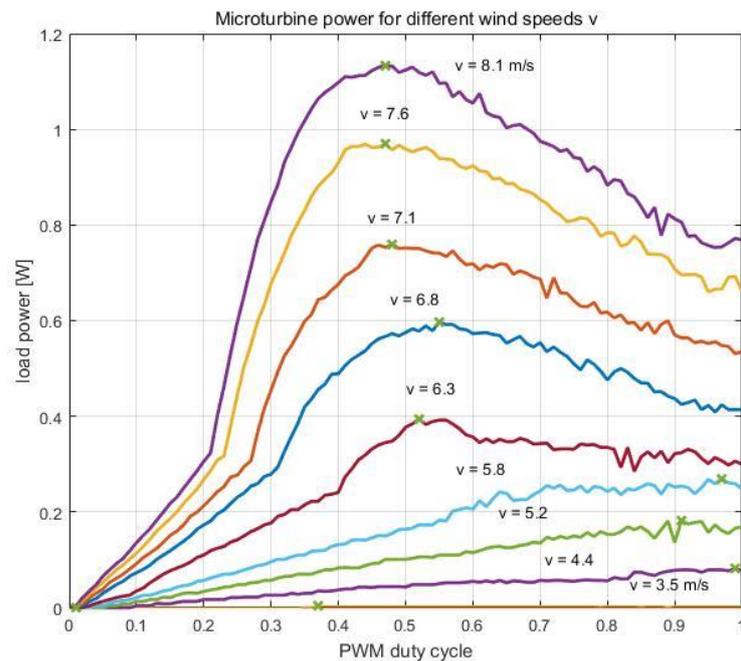
Figure 14. The power generated by a wind turbine with a constant pitch, as a function of the control value—duty cycle of the PWM signal, for different wind speeds.

On the other hand, Figure 15 shows the power characteristics obtained in the tests carried out on a wind turbine with adjustable pitch depending on the rotation speed n [rpm] of the turbine $\beta(n) = 30^\circ - n/150$, as a function of the duty cycle of the PWM signal for various wind speeds. It is worth noting that for a non-linear load such as a Li-Po cell, optimal operation of the power plant requires a wider range of PWM control variable values in the range $(0.45 \div 0.95)$. It is also necessary to take into account changes in the EMF voltage of the cell depending on the degree of its charge.

Figure 15. The power generated by a wind turbine with adjustable pitch, as a function of the duty cycle, for different wind speeds.

Figure 16 compares the obtained two characteristics of the maximum turbine power achieved as a function of wind speed for the case of fixed (β = *const*) and adjustable angle of the pitch (β = *f(n)*) of turbine blades. It can be seen that for the case of the adjustable angle of the pitch, the efficiency of the power plant is higher. In the experiment, the turbine achieves a high value of tip speed ratio $\lambda \approx 10$; the blades of the turbine are positioned almost perpendicular to the direction of the wind. In addition, taking into account the static friction of bearings and brushes and the cogging torque resulting from changes in the reluctance of the generator's magnetic circuit, the start-up of such a turbine is very difficult and takes place only at a relatively high wind speed of 4 m/s, compared to the wind speed of 1.5 m/s at which it stops. Adjusting the pitch angle of the blades can greatly facilitate the start-up of a wind turbine and allow it to operate at lower wind speeds. In addition, through the appropriate selection of the dependence β = *f(n)*, it is also possible to limit the maximum rotational speed of the turbine at which $\beta(n_{max})$ = 0.
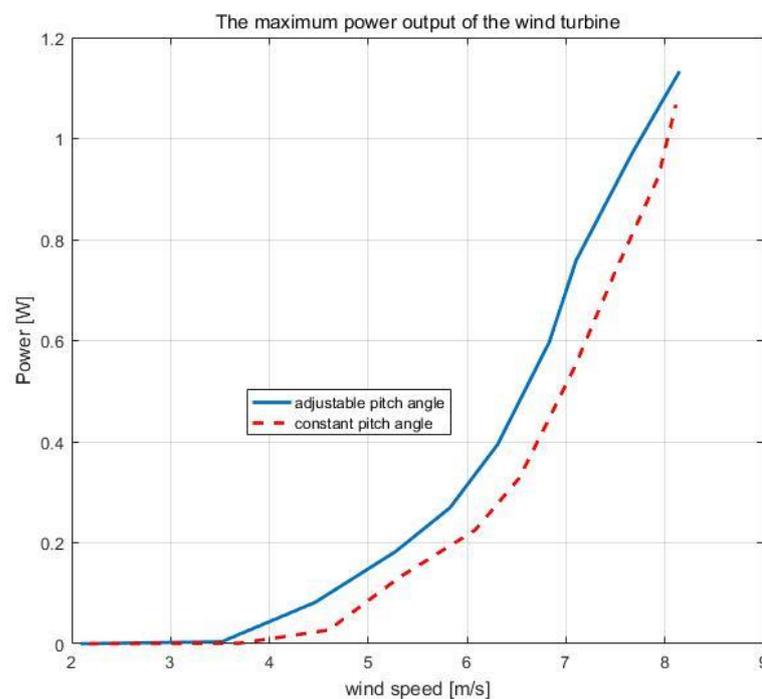
Figure 16. The maximum power of a wind microturbine for the case of constant and adjustable pitch.

The results of the measurements indicate that the direct connection of the battery to the generator, often used in wind microturbines, whose charging characteristics is strongly non-linear and changes depending on the battery charge level, may be the cause of poorer performance of the microturbine. The solution to this problem may be the use of a possibly simple converter that could linearize the load characteristics of the microturbine.

Tests were carried out of a wind microturbine model, controlled by an HCS algorithm, presented in Figure 6. Figure 17 shows selected results of the experiment in the form of graphs: power of the wind farm, value of the PWM duty factor, and the rotation speed of the turbine. The results were obtained at constant wind speed v = 6.5 m/s.
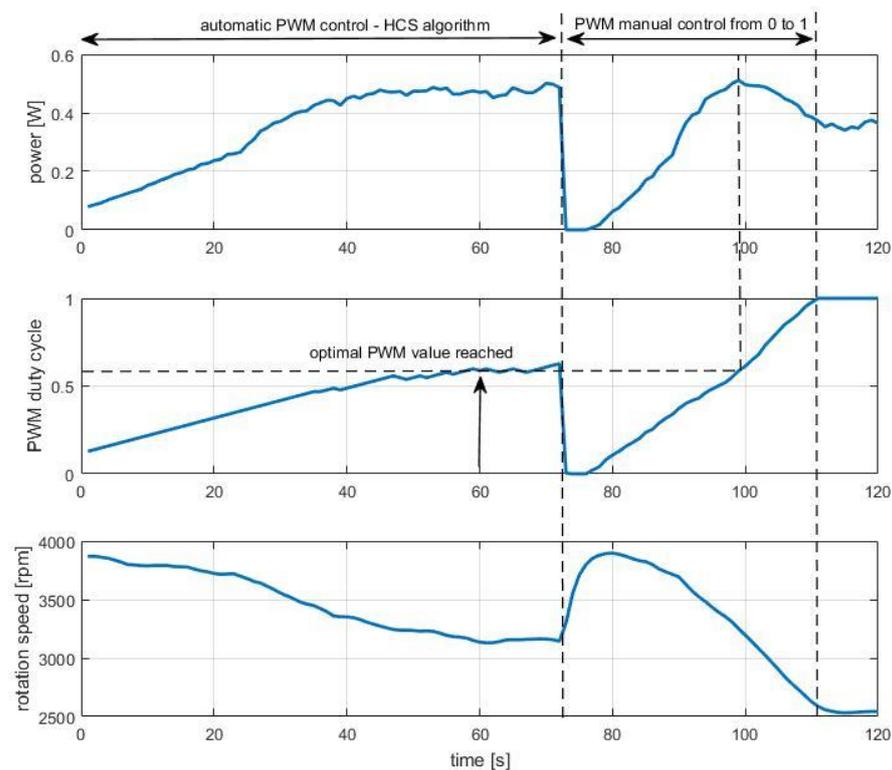
Figure 17. Graphs: microturbine power, duty factor PWM, and turbine rotation speed of a microturbine model controlled by HCS algorithm for adjustable pitch angle of the turbine blade.

The obtained results of the experiment show the possibility of using a simple HCS algorithm to control the operation of a wind microturbine only for a stable value of wind speed. In the case of rapid and greater decreases in wind speed, the presented simple HCS algorithm no longer works optimally, leading to a significant decrease in the turbine's rotational speed and its re-acceleration. A slight improvement in operation can be achieved in this case by using a simple mechanism for adjusting pitch angle of the blade $\beta = f(n)$, which prevents sudden stalling and facilitates the acceleration of the turbine. Some improvement can also be obtained by introducing additional actions to the control algorithm resulting from additional measurement of the instantaneous rotational speed of the turbine.

4. Conclusions

The obtained measurement results showed that the direct connection of the battery to the generator may cause poorer efficiency of the wind microturbine. The solution to this problem may be the use of a simple converter, which can linearize the load characteristics of the wind microturbine. The possibility of changing the pitch of the wind turbine depending on its rotation speed gives some improvement in the efficiency of the wind microturbine. However, in practical implementation, the additional costs of manufacturing the blade pitch adjustment mechanism and its reliability in difficult environmental conditions related to icing should be taken into account. The use of a simple mechanism for adjusting the pitch of the turbine using the centrifugal force of the rotating mass may be beneficial for two-blade microturbines with a high tip speed ratio. Resigning from the third blade in the wind turbine in favor of the blade angle adjustment mechanism, it is possible to achieve a higher rotational speed of the turbine, and thus to use a cheaper generator with a smaller number of pole pairs. The DC brush motor with permanent magnets used in the model as a generator proved its usefulness. The additional resistance to movement caused by the brushes did not cause significant limitations at lower wind speeds. Research has shown that DC motors used in radiator fans from scrap cars can be used in micro wind turbines for recycling. The use of a simple DC/DC converter in this case would allow optimal

adjustment of the load characteristic to achieve the maximum power of the wind turbine in a wide range of wind speeds. The conducted research showed that the built model of the wind microturbine allows us to observe and measure the physical phenomena related to the aerodynamics of the wind turbine and the operation of the electricity generator. Test results that use only simplified mathematical models of the wind turbine often do not take into account the phenomenon of stalling, which is significant when the maximum load power of the wind turbine for a given wind speed is exceeded.

The research model in the presented scale allows you to quickly and cheaply make and test initial prototypes of the designed wind turbine blades using popular 3D printers. In addition, the controller made enables the implementation, in the program memory of the used STM32F1 microcontroller, the developed algorithms for optimal control of the wind microturbine. The computing power of the 32-bit microcontroller is sufficient even for more complex algorithms. The specificity of the operation, construction, and limitations of micro wind turbines is in some aspects completely different than in the case of larger wind turbines, for which numerous scientific studies have already been prepared.

Due to the growing demand for autonomous and portable hybrid micro power plants, combining small photovoltaic panels and wind micro turbines, it is advisable to conduct research on improving the energy efficiency of these devices [6–8].

Further research work will focus on the use of the PMSG permanent magnet synchronous generator, the start-up of a wind microturbine with a high tip speed ratio, and algorithms for optimal MPPT control of the wind microturbine.

Conflicts of Interest: The author declares no conflict of interest.

References

1. Wu, Q.; Sun, Y. (Eds.) *Modeling and Modern Control of Wind Power*; John Wiley & Sons: Chichester, UK, 2018.
2. Bianchi, F.; De Battista, H.; Mantz, R. *Wind Turbine Control Systems. Principles, Modelling and Gain Scheduling Design*; Springer: London, UK, 2007.
3. Kadri, A.; Marzougui, H.; Bacha, F. MPPT control methods in wind energy conversion system using DFIG. In Proceedings of the 4th International Conference on Control Engineering & Information Technology (CEIT), Hammamet, Tunisia, 16–18 December 2016; pp. 1–6.
4. Zammit, D.; Spiteri Staines, C.; Micallef, A.; Apap, M. MPPT with Current Control for a PMSG Small Wind Turbine in a Grid-Connected DC Microgrid. In *Wind Energy Exploitation in Urban Environment*; Battisti, L., Ricci, M., Eds.; Springer International Publishing: Berlin/Heidelberg, Germany, 2018; pp. 205–219.
5. Carbon Trust. *Small-Scale Wind Energy: Policy Insights and Practical Guidance*; Carbon Trust: London, UK, 2008.
6. Juma, M.I.; Mwinyiwiwa, B.M.M.; Msigwa, C.J.; Mushi, A.T. Design of a Hybrid Energy System with Energy Storage for Standalone DC Microgrid Application. *Energies* **2021**, *14*, 5994. [CrossRef]
7. Mohamed, S.A.; Tolba, M.A.; Eisa, A.A.; El-Rifaie, A.M. Comprehensive Modeling and Control of Grid-Connected Hybrid Energy Sources Using MPPT Controller. *Energies* **2021**, *14*, 5142. [CrossRef]
8. Al-Quraan, A.; Al-Qaisi, M. Modelling, Design and Control of a Standalone Hybrid PV-Wind Micro-Grid System. *Energies* **2021**, *14*, 4849. [CrossRef]
9. Rolak, M.; Kot, R.; Malinowski, M.; Goryca, Z.; Szuster, J. AC/DC converter with maximum power point tracking algorithm for complex solution of small wind turbine. *Prz. Elektrotech.* **2011**, *87*, 91–96. (In Polish)
10. Shankareppagol, L.; Hampannavar, S.; Doadamani, S. Performance Analysis of P&O and INC MPPT for WECS. In Proceedings of the 3rd International Conference for Convergence in Technology (I2CT), Pune, India, 6–8 April 2018; pp. 1–8.
11. Baran, J.; Jąderko, A. Układ sterowania turbiny wiatrowej o regulowanej prędkości obrotowej i stałym kącie ustawienia łopat z liniowym obserwatorem momentu aerodynamicznego. *Prz. Elektrotech.* **2017**, *93*, 59–62. (In Polish) [CrossRef]
12. Chudzik, S. Stanowisko pomiarowe do testowania modeli mikroelektrowni wiatrowych. *Prz. Elektrotech.* **2021**, *97*, 154–157. (In Polish) [CrossRef]
13. Schubel, P.; Crossley, R. Wind turbine blade design. *Energies* **2012**, *5*, 3425–3449. [CrossRef]
14. Pande, J.; Nasikkar, P.; Kotecha, K.; Varadarajan, V. A Review of Maximum Power Point Tracking Algorithms for Wind Energy Conversion Systems. *J. Mar. Sci. Eng.* **2021**, *9*, 1187. [CrossRef]

15. Majout, B.; El Alami, H.; Salime, H.; Zine Laabidine, N.; El Mourabit, Y.; Motahhir, S.; Bouderbala, M.; Karim, M.; Bossoufi, B. A Review on Popular Control Applications in Wind Energy Conversion System Based on Permanent Magnet Generator PMSG. *Energies* **2022**, *15*, 6238. [CrossRef]

16. Abdullah, M.A.; Yatim, A.H.M.; Tan, C.W.; Saidur, C.W. A review of maximum power point tracking algorithms for wind energy systems. Renew. Sustain. *Energy Rev.* **2012**, *16*, 3220–3227.

17. Calabrese, D.; Tricarico, G.; Brescia, E.; Cascella, G.L.; Monopoli, V.G.; Leuzzi, R. Variable Structure Control of a Small Ducted Wind Turbine in the Whole Wind Speed Range Using a Luenberger Observer. *Energies* **2020**, *13*, 4647. [CrossRef]

18. Bekiroglu, E.; Yazar, M.D. MPPT Control of Grid Connected DFIG at Variable Wind Speed. *Energies* **2022**, *15*, 3146. [CrossRef]

19. Kim, J.-S.; Chung, I.-Y.; Moon, S.-I. Tuning of the PI controller parameters of a PMSG wind turbine to improve control performance under various wind speeds. *Energies* **2015**, *8*, 1406–1425. [CrossRef]

20. Bubalo, M.; Bašić, M.; Vukadinović, D.; Grgić, I. Experimental Investigation of a Standalone Wind Energy System with a Battery-Assisted Quasi-Z-Source Inverter. *Energies* **2021**, *14*, 1665. [CrossRef]

21. Yaakoubi, A.E.; Amhaimar, L.; Attari, K.; Harrak, M.; Halaoui, M.; Asselman, A. Non-linear and intelligent maximum power point tracking strategies for small size wind turbines: Performance analysis and comparison. *Energy Rep.* **2019**, *5*, 545–554. [CrossRef]

22. Aissaoui, H.E.; Ougli, A.E.; Tidhaf, B. Neural Networks and Fuzzy Logic Based Maximum Power Point Tracking Control for Wind Energy Conversion System. *Adv. Sci. Technol. Eng. Syst. J.* **2021**, *6*, 586–592. [CrossRef]

23. Syahputra, R.; Soesanti, I. Performance Improvement for Small-Scale Wind Turbine System Based on Maximum Power Point Tracking Control. *Energies* **2019**, *12*, 3938. [CrossRef]

24. Priyadarshi, N.; Ramachandaramurthy, V.K.; Padmanaban, S.; Azam, F. An Ant Colony Optimized MPPT for Standalone Hybrid PV-Wind Power System with Single Cuk Converter. *Energies* **2019**, *12*, 167. [CrossRef]

25. Daili, Y.; Gaubert, J.P.; Rahmani, L. Implementation of a new maximum power point tracking control strategy for small wind energy conversion systems without mechanical sensors. *Energy Convers. Manag.* **2015**, *97*, 298–306. [CrossRef]

26. Nandi, T.N.; Brasseur, J.; Vijayakumar, G. Prediction and Analysis of the Nonsteady Transitional Boundary Layer Dynamics for flow over an Oscillating Wind Turbine Airfoil using the γ-Reθ Transition Model. In Proceedings of the 34th Wind Energy Symposium, San Diego, CA, USA, 4–8 January 2016. [CrossRef]

27. Liu, J.; Xiao, Z.; Fu, S. Unsteady Transition Studies over a Pitching Airfoil Using a k-ω-γ Transition Model. *AIAA J.* **2018**, *56*, 3776–3781. [CrossRef]